

Constant False Alarm Rate Detectors in Intensive Noise Environment Conditions

Lyubka Doukovska

Institute of Information and Communication Technologies, 1113 Sofia

E-mail: doukovska@iit.bas.bg

Abstract: *A different technique of CFAR detectors procedure for moving target detection in noise environment conditions with a Poisson distributed flow and Raleigh amplitude distribution is proposed in this paper . The expressions of the detection and false alarm probability are derived for a highly fluctuating Swerling II target. A comparative analysis of the performance of different radar detectors structures keeping constant false alarm rates is done. These are a CA CFAR (Cell Averaging Constant False Alarm Rate), an EXC CFAR (EXCision Constant False Alarm Rate), a CFAR BI (Constant False Alarm Rate with Binary Integration), an EXC CFAR BI (EXCision Constant False Alarm Rate with Binary Integration) and an API CFAR (Adaptive censoring Post detection Integration Constant False Alarm Rate). A method for losses estimation, which allows choosing of optimal detector parameters, is developed. The estimates are obtained of the effectiveness of CFAR detectors in noise environment conditions and they are compared to patterns, investigated by other authors. The results achieved can be successfully applied for radar target detection and in the existing communication network receivers, that use pulse signals.*

Keywords: *Radar detector, CFAR detector, noise environment, randomly arriving impulse interference, probability of detection, probability of false alarm, detectability profits (losses).*

1. Introduction

Modern radio-systems function in complex electromagnetic environment, under conditions of created artificial and natural interference with unknown or variable parameters. That is usually mutual interference, from adjacent radio-electronic

devices, as a rule powerful and appearing casually, i.e., having noise environment characteristics with large intensity. This concerns especially signals from similar radars for air traffic control. Randomly Arriving Impulse Interference (RAII), in such cases, is received not only at the basic radar antenna channel, but also at the sidelobe and the backlobe diagram of the antenna, and receiving is possible not only at the basic frequency channel.

Signal detection in noisy or clutter environments is a very important part of target detection procedure. In theory the noise and clutter background will be described by a statistical model with e.g. Rayleigh, or exponentially distributed random variables of known average noise power. But in practical applications this average noise or clutter power is absolutely unknown and some statistical parameters can additionally vary over range, time and azimuth. In automatic radar detection, the signal received is sampled in range and frequency. Each sample is placed in an array of range and Doppler resolution cells. The clutter background in the cell under test is estimated by averaging the outputs of the nearby resolution cells (range and/or Doppler). The target detection is declared, if the signal value exceeds a preliminary determined threshold. Current estimating of the noise level in the reference window forms the threshold. The detection threshold is obtained by scaling the noise level estimate with a constant T_α to achieve a desired probability of false alarm P_{FA} .

As an estimate of the noise level, the estimate proposed by Finn and Johnson in [1] is quite often used. Averaging the outputs of the reference cells surrounding the test cell forms this estimate. Thus a constant false alarm rate is maintained in the process of detection. This is the conventional Cell Averaging Constant False Alarm Rate (CA CFAR) detector, proposed by Finn and Johnson in [1]. These CA CFAR processors are very effective in case of stationary and homogeneous interference and are effective almost as the ideal Neyman-Pearson detector, when the number of reference cells becomes very large. The presence of strong randomly arriving impulse interference in both, the test resolution cell and the reference cells, can cause drastic degradation in the performance of CA CFAR processor. Such type of interference is non-stationary and non-homogenous and is often caused by adjacent radar or other radio-electronic devices. In a non-homogenous environment, the detection performance and the false alarm regulation properties of CA CFAR detector may be seriously degraded.

During the last few years a lot of different approaches have been proposed to improve the detectability of CFAR detectors operating in random impulse noise [2-9]. One way for keeping constant false alarm rate under these conditions is the using of the excision CFAR detector presented in papers [11, 12], but it is not effective enough. More effective for the stabilization of false alarm is the implementation of Post-detection Integration (PI), and Binary Integration (BI) in CFAR signal processors, studied and analyzed in papers [5, 9]. Most effective is the Adaptive Post-detection Integrator CFAR (API CFAR) signal processor with adaptive selection on impulse noise in reference and in test windows and a post-detection integration procedure [5, 13].

The noise in test cells is a Rayleigh envelope distributed and target returns are fluctuating according to Swerling II model in [2-4]. Impulse noise exists only in the test window in [5], the average repetition frequency of pulse jamming in this case is determined by the number of pulses in a window. In references [7-10, 12] the authors assume that the samples of the total interference are distributed according to the compound exponential law, where the weighting coefficients are the probabilities of corrupting and non-corrupting of the samples. These probabilities for appearing of the impulse noise with average length in the cells of range depend on the multiplication of the average repetition frequency of impulse noise and the noise length.

In such situations it would be desirable to know the CFAR losses depending on the parameters of the impulse noise, for rating the behavior of the radar. There are two approaches for calculation of CFAR losses, offered by Rohling and Kassam in [2, 14]. The conventional method is to compute the additional SNR needed for CFAR processing scheme beyond that for the optimum processor, to achieve a fixed detection probability (e.g., 0.5), used in [5, 7-10, 12]. For a particular CFAR scheme the loss obviously varies with the detection probability. Alternatively, the authors in [2, 14] use another criterion, related to this one based on the Average Decision Threshold (ADT), since the threshold and the detection probability are closely related to one another. Then the difference between two CFAR systems in a homogeneous clutter situation is expressed by the ratio between the two ADT's measured in dB in [2, 14].

Such estimations and loss analysis are not described in [4, 5, 7]. On the other hand, in [8, 9, 12] the losses are estimated, but for a different value for the probability of detection 0.9755 and the results are compared with the same CFAR scheme in the situation without impulse noise. Similar investigation is presented in [2] and the results, which are achieved for CFAR processors, are equal to those presented in [2] for the case without impulse noise. Using the ADT approach and the Moment Generating Function (MGF) for modeling of the impulse noise is presented in [2]. The losses of CFAR detectors are calculated for different values of false alarm probability, for a different number of observations in the reference window, an average Interference-to-Noise Ratio (INR) and probabilities for appearance of impulse noise with average length in the cells in range.

The detection performance of CFAR processors is proposed by Hou in [2] for the case of homogeneous environment and chi-square family of fluctuating target models (Swerling I, II, III, and IV). In this paper the study is presented of the situation for a highly fluctuating target – Swerling II type target model detection under intensive noise environment conditions.

A comparative analysis of the performance of different types of CFAR detectors is carried out. This structure gives the possibility for keeping a constant false alarm rate in the presence of random arriving impulse interference. In this study one very interesting case is considered – the limit, when increasing the probability of the appearance changes the distribution law from Poisson to binominal. The binominal model is more general than Poisson distribution model

[3]. The change of the distribution law and the parameters of RAI leads to worsened detection process.

The research work is performed in MATLAB computational environment.

2. Signal model

Using the approach proposed in [1], new results are obtained for Swerling II type target detection model of performance in noise environment (Randomly Arriving Impulse Interference – RAI). The signal in the reference window is assumed to be with Poisson distribution and has the following Probability Density Function (PDF) [4]:

$$(1) \quad f_{sP}(x) = \frac{(1-e_0)}{\lambda_0(1+s)} \exp\left(\frac{-x}{\lambda_0(1+s)}\right) + \frac{e_0}{\lambda_0(1+s+r_j)} \exp\left(\frac{-x}{\lambda_0(1+s+r_j)}\right)$$

where s is the per pulse average Signal-to-Noise Ratio (SNR), λ_0 is the average power of the receiver noise, r_j is the average INR, e_0 is the probability of appearance of RAI.

Under conditions of binomial distribution of pulse interference, the probability of interference-plus-noise occurrence in the background environment is $2e_0(1-e_0)$. The probability of appearance of two interferences in a single cell is e_0^2 and having only noise probability is $(1-e_0)^2$, where $e_0 = 1 - \sqrt{1-t_c F}$, F is the average repetition frequency of pulse interference and t_c is the length of pulse transmission [4].

The distribution is binomial when the probability of pulse interference is above 0.1 [4]. In these situations the outputs of the reference window are observations from statistically independent exponential random variables. Consequently, the PDF of the reference window outputs may be defined by:

$$(2) \quad f_{sB}(x) = \frac{(1-e_0)^2}{\lambda_0(1+s)} \exp\left(\frac{-x}{\lambda_0(1+s)}\right) + \frac{2e_0(1-e_0)}{\lambda_0(1+s+r_j)} \exp\left(\frac{-x}{\lambda_0(1+s+r_j)}\right) + \frac{e_0^2}{\lambda_0(1+s+2r_j)} \exp\left(\frac{-x}{\lambda_0(1+s+2r_j)}\right)$$

where λ_0 is the average power of the receiver noise and r_j/λ_0 is the per pulse average INR.

In the next two figures, according to paper [15], comparative simulation examples are shown for Poisson and for binomial distributions of pulse interference, with signal and noise parameter values $-s = 70$ dB, $\lambda_0 = 1$, $r_j = 30$ dB, $e_0 = 0.1$.

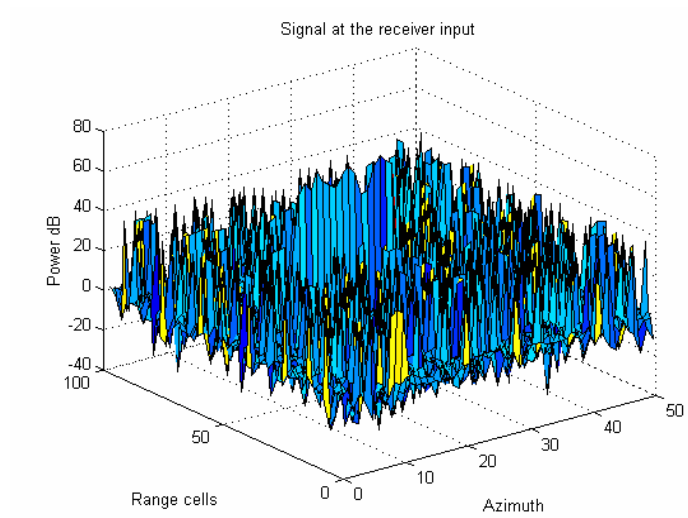


Fig. 1. Example of Poisson distribution of pulse interference

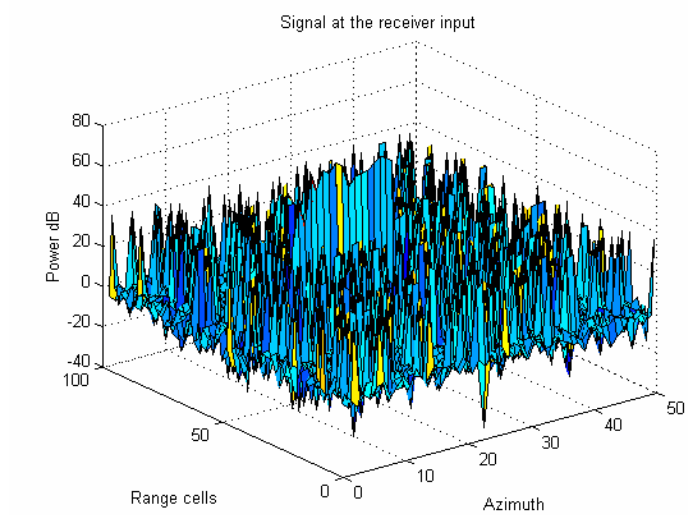


Fig. 2. Example of binominal distribution of pulse interference

3. CFAR processors statistical analysis

In the modern radars system, keeping constant false alarm rates, the target is detected according to the following algorithm [1]:

$$(3) \quad \begin{cases} H_1 : \Phi(q_0) = 1, q_0 > T_\alpha V \\ H_0 : \Phi(q_0) = 0, q_0 < T_\alpha V \end{cases}$$

where H_1 is the hypothesis that the test resolution cell contains the echoes from the target and H_0 is the hypothesis that the test resolution cell contains the randomly arriving impulse interference only, V is the noise level estimation. The constant T_a is a scale coefficient, which is determined in order to maintain a given constant false alarm rate.

The different CFAR structures make use of different algorithms for noise level estimation – V [5-14]. In this paper several types of signal processors are analyzed – a CA (Cell Averaging), an EXC (EXCision), a BI (Binary Integration), an EXC BI (EXCision with Binary Integration) and an API (Adaptive censoring Post detection Integration). On Fig. 3 one example is presented of the adaptive threshold procedure for one-dimensional CFAR processor in conditions of randomly arriving impulse interferences [15].

The general structure of an adaptive CFAR processor is shown on Fig. 4.

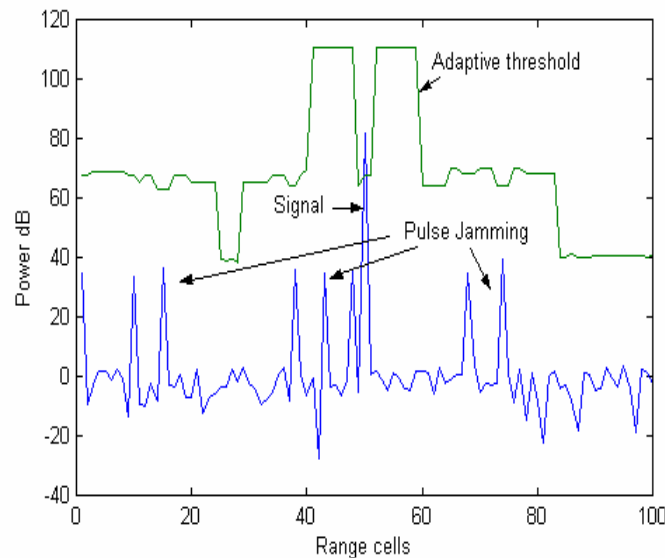


Fig. 3. Adaptive threshold procedure for one-dimensional CFAR processor

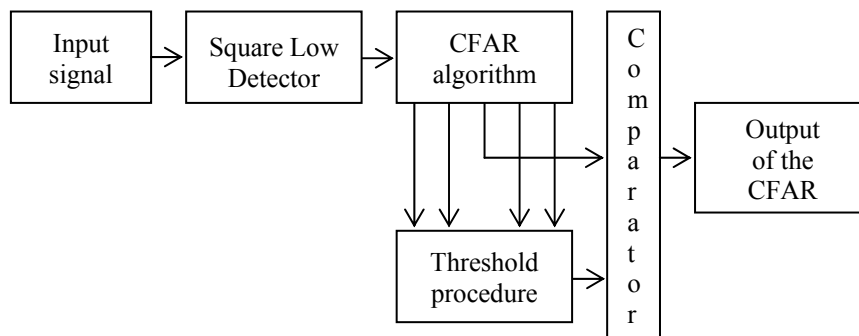


Fig. 4. General structure of an adaptive CFAR processor

Let us assume that L pulses hit the target, which is modeled according to Swerling II case. The signal received is sampled in range by using $N+1$ resolution cells resulting in a matrix with $N+1$ rows and L columns. Each column of the data matrix consists of the values of the signal obtained for L pulse intervals in one range resolution cell. Let us also assume that the first $N/2$ and the last $N/2$ rows of the data matrix are used as a reference window in order to estimate the “noise-plus-interference” level in the radar test resolution cell. In this case the samples of the reference cells result in a matrix X of size $N \times A$. The test cell or the radar target image includes the elements of the $N/2+1$ row of the data matrix and is a vector Z of length L .

The probability of detection for a CA CFAR processor for target of case Swerling II, according to [8] is

$$(4) \quad P_{D_{CA}} = \sum_{i=1}^N C_N^i e_0^i (1-e_0)^{N-i} \left\{ \frac{e_0}{\left(1 + \frac{(1+r_j)T_{CA}}{1+r_j+s}\right)^i \left(1 + \frac{T_{CA}}{1+r_j+s}\right)^{M-i}} + \frac{1-e_0}{\left(1 + \frac{(1+r_j)T_{CA}}{1+s}\right)^i \left(1 + \frac{T_{CA}}{1+s}\right)^{M-i}} \right\}$$

where T_{CA} is the threshold constant for CA CFAR processor.

The probability of detection for CFAR BI signal processor in this noise situation [9] is

$$(5) \quad P_{D_{BI}} = \sum_{i=0}^N C_N^i e_0^{2i} \sum_{j=0}^{N-i} C_{N-i}^j (2e_0(1-e_0))^j (1-e_0)^{2(N-i-j)} \{R_1 + R_2 + R_3\}$$

where:

$$R_1 = \frac{(1-e_0)^2}{\left(1 + \frac{T_{BI}(1+2r_j)}{1+r_j+s}\right)^i \left(1 + \frac{T_{BI}(1+r_j)}{1+r_j+s}\right)^j \left(1 + \frac{T_{BI}}{1+r_j+s}\right)^{N-i-j}},$$

$$R_2 = \frac{2e_0(1-e_0)}{\left(1 + \frac{T_{BI}(1+2r_j)}{1+r_j+s}\right)^i \left(1 + \frac{T_{BI}(1+r_j)}{1+r_j+s}\right)^j \left(1 + \frac{T_{BI}}{1+r_j+s}\right)^{N-i-j}},$$

$$R_3 = \frac{e_0^2}{\left(1 + \frac{T_{BI}(1+2r_j)}{1+2r_j+s}\right)^i \left(1 + \frac{T_{BI}(1+r_j)}{1+2r_j+s}\right)^j \left(1 + \frac{T_{BI}}{1+2r_j+s}\right)^{N-i-j}},$$

where T_{BI} is the threshold constant for CFAR BI processor.

For comparison on the next two figures, the outputs of CA CFAR and CFAR BI detectors are presented.

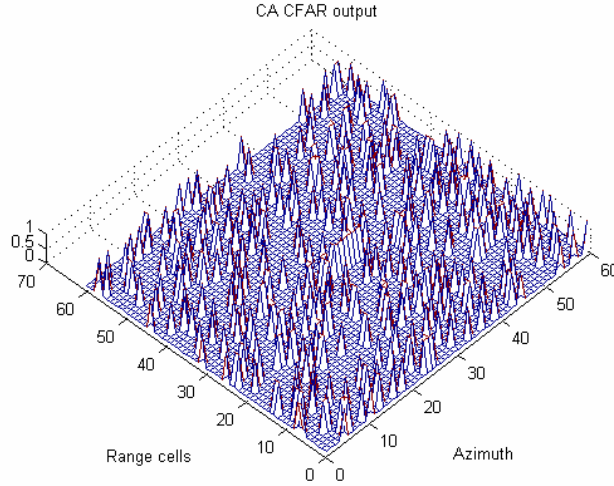


Fig. 5. Example of a CA CFAR output detector

The probability of detection for an EXC CFAR processor for target model Swerling II, according to [6] is

$$(6) \quad P_{D_{\text{EXC}}} = \sum_{k=1}^N C_N^k P_E^k (1 - P_E)^{N-k} \left\{ (1 - e_0) M_V \left(\frac{T_{\text{EXC}}}{\lambda_0(1+s)}, k \right) + e_0 M_V \left(\frac{T_{\text{EXC}}}{\lambda_0(1+r_j+s)}, k \right) \right\}$$

where $M_V(\cdot)$ is the Moment Generating Function (MGF) and T_{EXC} is a predetermined scale factor for EXC CFAR processor.

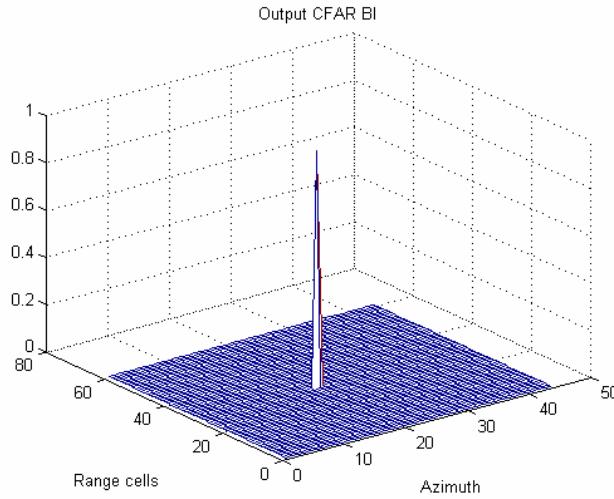


Fig. 6. Example of a CFAR BI output detector

The MGF of the noise level estimate V , may be obtained as

$$(7) \quad M_V(U) = \sum_{k=1}^N \binom{N}{k} P_E^k (1-P_E)^{N-k} M_V(U, k)$$

where $U = f(T_{\text{EXC}}, s, r_j, \lambda_0)$ and the probability that a sample x_i survives at the excision output is calculated as

$$(8) \quad P_E = 1 - (1 - e_0) \exp\left(\frac{-B_E}{\lambda_0}\right) - e_0 \exp\left(\frac{-B_E}{\lambda_0(1+r_j)}\right).$$

The function $M_V(U, k)$ is the conditional MGF of the estimate V where k is the number of samples survived at the excision output.

The probability of pulse train detection for EXC CFAR BI processors is evaluated in such noise situation as in [7, 11] by

$$(9) \quad P_{D_{\text{EXC BI}}} = \sum_{l=M}^L C_L^l P_{D_{\text{EXC}}}^*{}^l (1 - P_{D_{\text{EXC}}}^*)^{L-l}$$

where M is binary decision rule, $P_{D_{\text{EXC}}}$ is the probability of pulse detection, which may be found using the expressions for EXC CFAR processor with Poisson impulse noise.

In this one very effective CFAR detector case paper is considered, when both the two-dimensional reference window and the test cells are corrupted by randomly arriving impulse interference, whose average repetition frequency and magnitude are unknown, [13]. The censoring procedure given in [4, 5], in order to remove the unwanted samples from both the reference window and the test cell before forming the adaptive threshold and the test statistic, is used. In this case the numbers of the integrated samples in the test cell and also in the reference window are random variables with binomial distribution. According to the censoring algorithm all the elements with high intensity of signal are removed from the reference window and the test resolution cell. The censoring algorithm consists of the following stages:

Stage 1. The elements of the reference window $\vec{x} = (x_1, x_2, \dots, x_N)$ and the test resolution cell $\vec{z} = (z_1, z_2, \dots, z_L)$ are rank-ordered according to increasing magnitude,

$$(10) \quad x_1^{(1)} \leq x_2^{(1)} \dots \leq x_i^{(1)} \dots \leq x_N^{(1)} \text{ and } z_1^{(1)} \leq z_2^{(1)} \dots \leq z_j^{(1)} \dots \leq z_L^{(1)}.$$

Stage 2. Each of the so ranked elements is compared with the adaptive threshold, according to the following rule:

$$(11) \quad x_{i+1}^{(1)} \geq s_i^x T_i^x, i = 1, \dots, N-1, \text{ and } z_{j+1}^{(1)} \geq s_j^z T_j^z, j = 1, \dots, L-1,$$

where $s_i^x = \sum_{l=1}^i x_l^{(1)}$ and $s_j^z = \sum_{l=1}^j z_l^{(1)}$.

After the stop of the recursive procedure, it is assumed that most or all of the randomly arriving impulse interferences are in the second part of the reference window and the test resolution cell. In this paper is proposed the more general expression for the probability of target detection in the presence of Poisson distribution noise environment conditions may be calculated as in [13]:

$$\begin{aligned}
P_{D_{\text{API}}} = & \sum_{k=1}^N \binom{N}{k} (1-e_0)^k e_0^{N-k} \sum_{l=1}^L \binom{L}{l} (1-e_0)^l e_0^{L-l} \sum_{i=0}^{l-1} \binom{k+i-1}{i} \frac{T_{\text{API}}^i (1+s)^k}{(T_{\text{API}} + 1+s)^{k+i}} + \\
& + \sum_{k=1}^N \binom{N}{k} (1-e_0)^k e_0^{N-k} e_0^L \sum_{i=0}^{L-1} \binom{k+i-1}{i} T_{\text{API}}^i (1+r_j+s)^k (T_{\text{API}} + 1+r_j+s)^{-(k+i)} + \\
(12) \quad & + \sum_{l=1}^L \binom{L}{l} (1-e_0)^l e_0^{L-l} e_0^N \sum_{i=0}^{l-1} \binom{N+i-1}{i} T_{\text{API}}^i \left(\frac{1+s}{1+r_j} \right)^N \left(T_{\text{API}} + \frac{1+s}{1+r_j} \right)^{-(N+i)} + \\
& + e_0^N e_0^L \sum_{i=0}^{L-1} \binom{N+i-1}{i} T_{\text{API}}^i \left(\frac{1+r_j+s}{1+r_j} \right)^N \left(T_{\text{API}} + \frac{1+r_j+s}{1+r_j} \right)^{-(N+i)}
\end{aligned}$$

where T_{API} is a predetermined scale factor for API CFAR processor that provides a constant false alarm rate (P_{FA}).

The probability of false alarm for the CFAR processors with target model case Swerling II in randomly arriving impulse interference is obtained for value of signal-to-noise ratio $s = 0$.

For comparison and calculation of CFAR detector losses the ratios are used between two values of SNR for different CFAR processors, measured in dB. This approach is considered in [14]:

$$(13) \quad \Delta = 10 \log \frac{\text{SNR} \Big|_{\text{CFAR}_1}}{\text{SNR} \Big|_{\text{CFAR}_2}}, \text{ by } P_{\text{FA}} = \text{const}, P_{\text{D}} = P_{\text{D}}^{\text{CFAR}_1} = P_{\text{D}}^{\text{CFAR}_2} = 0.5.$$

4. Numerical results

It is proved in this paper that different CFAR processors used for signal detection on the homogeneous background of unknown intensity and in the presence of randomly arriving impulse interference with known parameters, improve the detection performance. In such CFAR processors it is usually assumed that the noise amplitude is a Rayleigh distributed variable and the power, therefore, is an exponentially distributed variable. The numerical results presented are obtained after detailed simulational analysis of CFAR detectors performance under noise environment conditions. The analysis of the performance of different structures of one-dimensional and two-dimensional CFAR signal processors – CA CFAR (cell average), EXC CFAR (excision), CFAR BI (binary integration), EXC CFAR BI (excision and binary integration) and API CFAR (adaptive post integration) is done.

The achieved results for CA CFAR detector threshold analysis with three values of the probability of false alarm (P_{FA}), for two values of number of observations in the reference window (N), for two values of average interference-to-noise ratio (INR) and for five different values for a probability of appearance of impulse interference with average length in the cells in range are presented in Table 1.

Table 1

e_0	P_{FA}	$N = 16$		$N = 32$	
		INR=10, dB	INR=30, dB	INR=10, dB	INR=30, dB
0	10^{-4}	0.778	0.778	0.334	0.334
	10^{-6}	1.37	1.37	0.54	0.54
	10^{-8}	2.16	2.16	0.778	0.778
0.01	10^{-4}	3.56	320	1.63	143
	10^{-6}	8.4	761	3.56	320
	10^{-8}	14.85	1345	5.805	524
0.033	10^{-4}	4.41	389	1.925	159
	10^{-6}	9.5	845	3.86	338
	10^{-8}	16.3	1472	6.125	546
0.066	10^{-4}	4.68	400	1.94	144.5
	10^{-6}	9.8	869	3.818	321
	10^{-8}	16.68	1493	6.04	526
0.1	10^{-4}	4.67	386	1.845	117
	10^{-6}	9.72	849	3.635	290
	10^{-8}	16.54	1465	5.79	489

The probability of detection for CA CFAR detector is shown on Fig. 7 for constant detection threshold achieved for non homogeneous interference with parameters – average power of the receiver noise $\lambda_0 = 1$, average INR $r_j = 30$ dB, probability of appearance of impulse interference with average length in the range cells $e_0 = 0 \div 0.1$.

The results for EXC CFAR detector threshold analysis with probability of false alarm ($P_{FA} = 10^{-4}$), excision constant – $B_E = 2$, for two values of number of observations in the reference window (N), an average interference-to-noise ratio (INR = 30 dB) and nine different values for probability of appearance of impulse interference with average length in the cells in range are presented in Table 2.

The probability of detection for EXC CFAR detector is shown on Fig. 8. The study is analyzed for constant detection threshold achieved for non homogeneous interference with parameters – average power of the receiver noise $\lambda_0 = 1$, average INR $r_j = 30$ dB, probability of appearance of impulse interference with average length in the range cells $e_0 = 0.1 \div 0.9$.

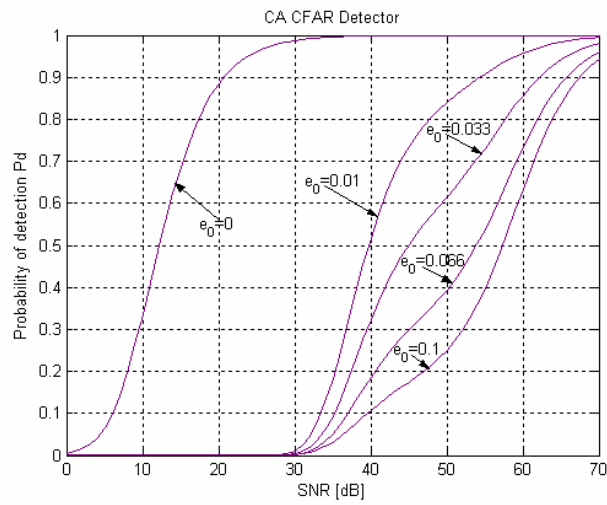


Fig. 7. Probability of detection for CA CFAR detector

Table 2

e_0	$N=16$	$N=32$
0.1	12 750	11 602
0.2	15 655	14 026
0.3	18 185	15 820
0.4	21 215	17 236
0.5	28 265	18 562
0.6	68 176	20 321
0.7	293 988	25 673
0.8	1 105 999	115 599
0.9	2 745 555	1 266 299

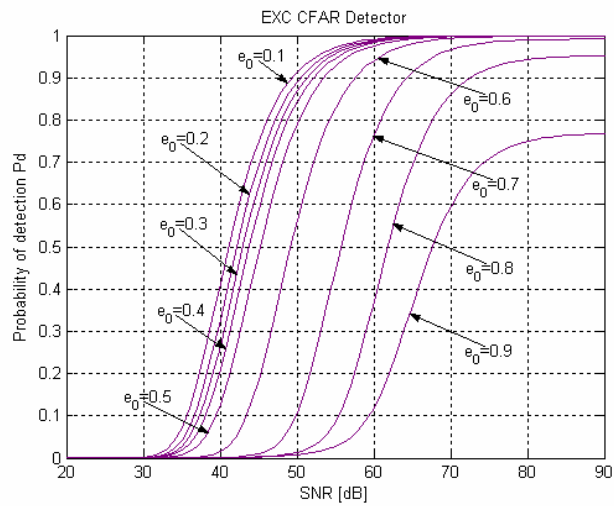


Fig. 8. Probability of detection for EXC CFAR detector

Table 3 presents the obtained threshold constants under equal experimental conditions for the different CFAR detection structure with two-dimensional binary integration procedure. The results are achieved for a value of probability of false alarm ($P_{FA} = 10^{-4}$), for two values of binary rules – 10/16 and 16/16, for nine values of probability of appearance of impulse interference and an average interference-to-noise ratio (INR=30 dB).

Table 3

e_0	$M/L=10/16$	$M/L=16/16$
0.1	0.0458	0.000316
0.2	0.1295	0.0002168
0.3	0.1367	0.000294
0.4	0.13147	0.0117
0.5	0.1255	0.02228
0.6	0.12088	0.02778
0.7	0.11763	0.03098
0.8	0.11547	0.03314
0.9	0.1140	0.0349

The probabilities of detection for CFAR BI detector with two different values of binary rules on next two figures – Fig. 9 ($M/L=10/16$) and Fig. 10 ($M/L=16/16$) are presented. The results are achieved for the following parameters - probability of false alarm $P_{FA} = 10^{-4}$, average power of the receiver noise $\lambda_0=1$, average INR $r_j=30$ dB, probability of appearance of impulse interference with average length in the range cells $e_0 = 0.1 \div 0.9$.

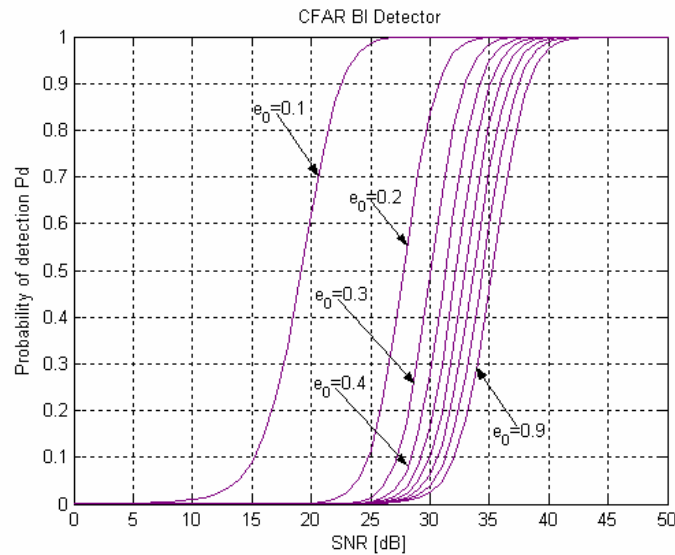


Fig. 9. Probability of detection for CFAR BI detector

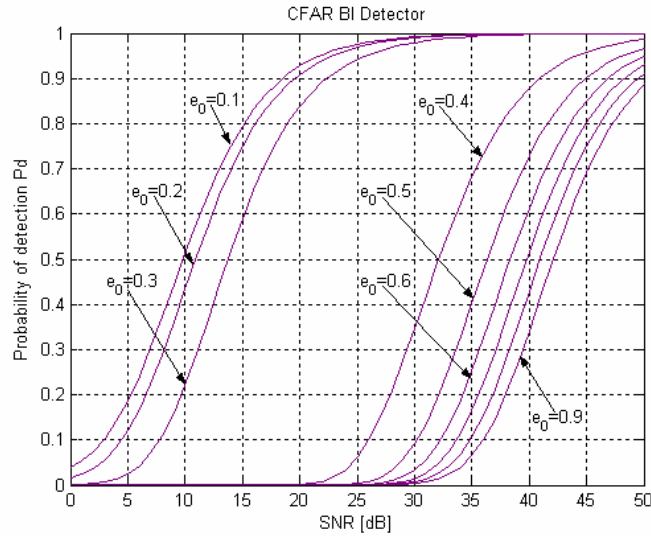


Fig. 10. Probability of detection for CFAR BI detector

Table 4 presents the obtained threshold constant values under equal experimental conditions for the two-dimensional EXC CFAR BI detector. The results are achieved for value of probability of false alarm ($P_{FA}=10^{-4}$), for two values of binary rules – 10/16 and 16/16, for nine values of probability of appearance of impulse interference and an average interference-to-noise ratio (INR=30 dB).

Table 4

e_0	$M/L=10/16$	$M/L=16/16$
0.1	7.1162	1.8831
0.2	142.7784	2.1544
0.3	697.8724	2.5797
0.4	1093.3	3.3448
0.5	1415.9	5.2840
0.6	1715.9	82.8785
0.7	2038.0	279.3980
0.8	2409.5	420.8292
0.9	2566.7	304.9783

The probabilities of detection for EXC CFAR BI detector with two different values of binary rules on next two figures – Fig. 11 ($M/L=10/16$) and Fig. 12 ($M/L=16/16$) are presented. The results are achieved for the following parameters – probability of false alarm $P_{FA}=10^{-4}$, excision constant $B_E=2$, average power of the receiver noise $\lambda_0=1$, average INR $r_j=30$ dB, probability of appearance of impulse interference with average length in the range cells $e_0=0.1\div 0.9$.

The numerical results for the obtained threshold constants values in equal experimental conditions for the two-dimensional API CFAR detector are included

in Table 5. The results are achieved for three values of probability of false alarm (P_{FA}), for two values of numbers of observations in the reference window (N, L), for two values of average INR and for five different values for a probability of appearance of impulse interference with average length in the cells in range.

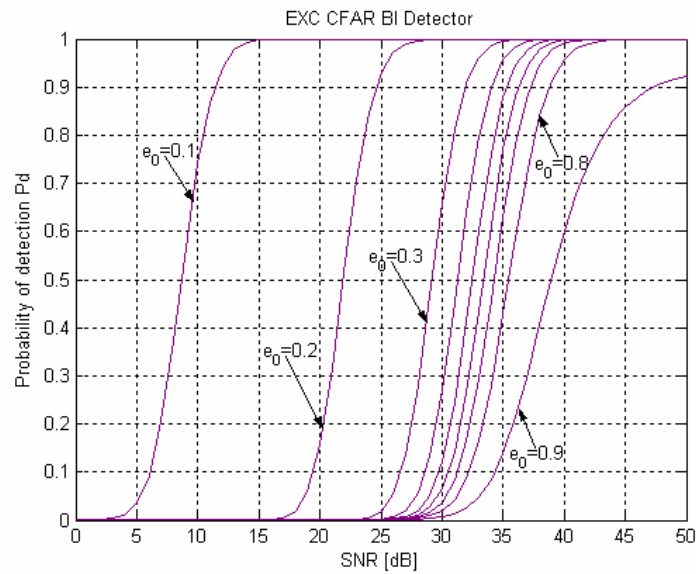


Fig. 11. Probability of detection for EXC CFAR BI detector

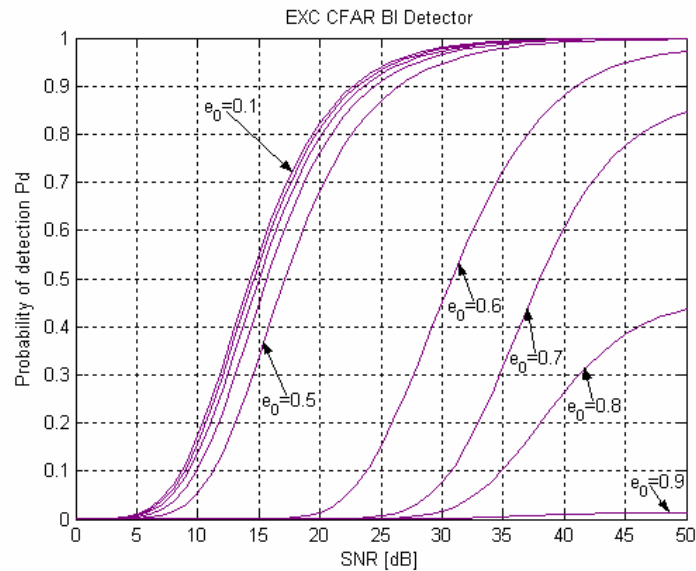


Fig. 12. Probability of detection for EXC CFAR BI detector

Table 5

e_0	P_{FA}	$N=16$ and $L=16$	$N=16$ and $L=32$
		INR = 10 dB and INR = 30 dB	INR = 10 dB and INR = 30 dB
0	10^{-4}	3.950	7.0878
	10^{-6}	6.0233	10.6250
	10^{-8}	8.7413	15.2578
0.01	10^{-4}	4.0533	7.2873
	10^{-6}	6.2484	11.0587
	10^{-8}	9.1995	16.1383
0.033	10^{-4}	4.309	7.7822
	10^{-6}	6.8228	12.1659
	10^{-8}	10.4148	18.4768
0.066	10^{-4}	4.7278	8.5935
	10^{-6}	7.8151	14.0819
	10^{-8}	12.6774	22.8404
0.1	10^{-4}	5.2377	9.5826
	10^{-6}	9.1142	16.5961
	10^{-8}	15.9710	29.2174

The probabilities characteristics of detection for API CFAR detector are shown on Fig. 13 for constant detection threshold achieved for non homogeneous interference with parameters – probability of false alarm ($P_{FA} = 10^{-4}$), for values of number of observations in the reference window ($N = 16, L = 16$), an average interference-to-noise ratio (INR=30 dB) and five different values for probability of appearance of impulse interference with average length in the cells in the range $e_0 = 0 \div 0.1$.

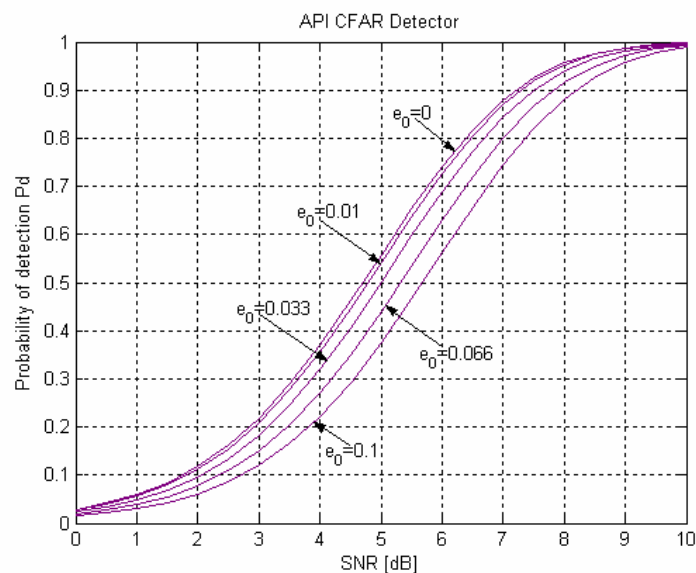


Fig. 13. Probability of detection for API CFAR detector

5. Conclusions

The experimental results reveal the influence of the interference on the detection process, when having constant false alarm rate in noise environment conditions. The paper presented considers the results obtained by the proposed adaptive threshold determination procedure and the analysis of different CFAR detector structures in intensive randomly arriving impulse interference environment. The need for an adequate threshold analysis procedure, enabling better detection results for low values of SNR, is considered.

The value of the test resolution cell and the probability of false alarm over the average detection threshold are studied. The application of censoring techniques in the detection algorithm improves the CFAR detectors effectiveness.

The results obtained may have significant practical application for CFAR detectors working under noise environment conditions. The obtained results show, that the API CFAR (Adaptive censoring Post detection Integration CFAR) processor is the most effective in these conditions.

As a final conclusion the results achieved in the presented paper confirm once again the necessity for synthesis of new algorithms for moving targets detection, assuring robustness and higher efficiency of the radar systems. The results obtained in this paper could practically be used in radar and communication networks.

References

1. Finn, H., R. Johnson. Adaptive Detection Mode with Threshold Control as a Function of Spatially Sampled Clutter Estimation. – RCA Review, Vol. **29**, 1968, No 3, 412-464.
2. Hou, X., N. Morinaga, T. Namekawa, Direct Evaluation of Radar Detection Probabilities. – IEEE Trans., Vol. **AES-23**, 1987, No 4, 418-423.
3. Goldman, H., I. Bar-David. Analysis and Application of the Excision CFAR Detector. – In: IEE Proc., Vol. **135**, Pt.F, 1988, No 6, 563-575.
4. Kabakchiev, C., L. Doukovska, I. Garvanov. Hough Radar Detectors in Conditions of Intensive Pulse Jamming. – Sensors & Transducers Magazine, Special Issue “Multisensor Data and Information Processing”, 2005, 381-389.
5. Kabakchiev, C., I. Garvanov, L. Doukovska. Adaptive Censoring CFAR PI Detector with Hough Transform in Randomly Arriving Impulse Interference. – Cybernetics and Information Technologies, Vol. **5**, 2005, No 1, 115-125.
6. Kabakchiev, C., I. Garvanov, L. Doukovska. Excision CFAR BI Detector with Hough Transform in Presence of Randomly Arriving Impulse Interference. – In: Proc. of the International Radar Symposium – IRS’05, Berlin, Germany, 2005, 259-264.
8. Doukovska, L., C. Kabakchiev. Performance of Hough Detectors in Presence of Randomly Arriving Impulse Interference. – In: Proc. of the International Radar Symposium – IRS’06, Krakow, Poland, 2006, 473-476.
8. Kabakchiev, C., L. Doukovska, I. Garvanov. Cell Averaging Constant False Alarm Rate Detector with Hough Transform in Randomly Arriving Impulse Interference. – Cybernetics and Information Technologies, Vol. **6**, 2006, No 1, 83-89.
9. Doukovska, L. Hough Detector with Binary Integration Signal Processor. Compt. Rend. Acad. Bulg. Sci., Vol. **60**, 2007, No 5, 525-533.
10. Doukovska, L., V. Behar, C. Kabakchiev. Hough Detector Analysis by means of Monte Carlo Simulation Approach. – In: Proc. of the International Radar Symposium – IRS’08, Wroclaw, Poland, 2008, 103-106.

11. Doukovska, L. Moving Target Hough Detector in Pulse Jamming. – Cybernetics and Information Technologies, Vol. 7, 2007, No 1, 67-76.
12. Doukovska, L. Hough Detector with One-dimensional CFAR Processors in Randomly Arriving Impulse Interference. – In: Proc. of Distributed Computer and Communication Networks, International Workshop, Sofia, Bulgaria, 2006, 241-254.
13. Behar, V., Kabakchiev, L. Doukovska. Adaptive CA CFAR Processor for Radar Target Detection in Pulse Jamming. – Journal of VLSI Signal Processing, Vol. 26, 2000, 383-396.
14. Rohling, H. Radar CFAR Thresholding in Clutter and Multiple Target Situation. – IEEE Transaction, Vol. AES-19, 1983, No 4, 608-621.
15. Doukovska, L., I. Garvanov. Hough Detector Threshold Analysis in Presence of Randomly Arriving Impulse Interference. – Cybernetics and Information Technologies, Vol. 10, 2010, No 1, 37-48.